Ethanol Extract from *Astilbe Chinensis* Inflorescence Suppresses Inflammation in Macrophages and Growth of Key Oral Pathogenic Bacteria

Jong Min Han
Docsmedi Corp.
Ina Yun
Apple Tree Institute of Biomedical Science, Apple Tree Dental Hospitial
Kyung Mi Yang
Apple Tree Institute of Biomedical Science, Apple Tree Dental Hospitial
Hye-Sung Kim
Apple Tree Institute of Biomedical Science, Apple Tree Dental Hospitial
Young-Youn Kim
Apple Tree Institute of Biomedical Science, Apple Tree Dental Hospitial
Wonsik Jeong
Bio-Center, Gyeonggido Business & Science Accelerator (GBSA)
Seong Su Hong
Bio-Center, Gyeonggido Business & Science Accelerator (GBSA)
Inseong Hwang (inseong.hwang@gmail.com)
Docsmedi Corp.

Research Article

Keywords: Ethanol, Inflorescence, Suppresses Inflammation, Macrophages, Key, Pathogenic Bacteria, pathological causes, oral diseases, dental diseases

Posted Date: September 24th, 2021

DOI: https://doi.org/10.21203/rs.3.rs-900522/v1

Abstract

Dysregulation of infection-derived inflammatory responses has been one of the crucial pathological causes of oral diseases. Even though the organic extracts of *Astilbe chinensis* have been frequently reported to have anti-inflammatory activity, the study on the extract of *A. chinensis* inflorescence has yet to be reported. Here, we evaluated the anti-inflammatory efficacy of *A. chinensis* collected from a variety of regions and seasons and successfully demonstrated that GA-13-6, an ethanol extract of *A. chinensis* inflorescence collected in a flowering season, inhibited the production of inflammatory mediators and proinflammatory cytokines, such as nitric oxide (NO), tumor necrosis factor (TNF), and interleukin-6 (IL-6) and suppressed the expression of cyclooxygenase-2 (COX2) and inducible nitric oxide synthase (iNOS) both in mRNA and protein levels in lipopolysaccharide (LPS)-stimulated RAW 264.7 macrophages. Importantly, we for the first time confirmed that GA-13-6 efficiently inhibited the growth of *Porphyromonas gingivalis*, *Streptococcus sanguinis*, and *Streptococcus mutans*, showing that GA-13-6 possesses antibacterial activity against these pivotal oral pathogens. Thus, GA-13-6 is a potential active ingredient not only for the treatment or prevention of periodontal and dental diseases but many other inflammation-related diseases.

Introduction

Periodontal diseases and dental caries are the two most common oral diseases that lead to tooth loss[1]. Periodontal diseases, such as gingivitis and periodontitis, are caused by the accumulation of polymicrobial infections of the structures supporting the teeth, such as gingiva (gums), periodontal ligament, and alveolar bone. Chronic periodontitis begins with gingivitis, a localized reversible inflammation of the gingiva initiated by bacteria in a microbial biofilm[2]. One of the major pathogens in the biofilm includes *P. gingivalis*, an anaerobic, asaccharolytic, immotile Gram-negative bacterium ensconced in subgingival pockets[3–6]. Dental caries (cavities) is common biofilm-dependent tooth decay caused by a breakdown of the hard tissue of the teeth, enamel, dentin, and cementum because of acidic by-products (e.g., lactic acid) fermented by saccharolytic bacteria, such as *S. mutans* and *S. sanguinis*[7]. *S. mutans* and *S. sanguinis*, members of the phylum Firmicutes, are facultatively anaerobic, Gram-positive bacteria. *S. mutans* adheres to the supragingival delamination layer of the teeth, has higher acid tolerance than *S. sanguinis*, and is thus considered to be one of the major etiologic agents of the disease onset[8]. While *S. sanguinis* serves as a commensal bacterium abundant in a normal oral cavity, a dysbiosis of oral microbiota makes the bacterium an opportunistic pathogen. Thus, ecological balances of oral microflora are now getting much attention to understand the widespread diseases. Furthermore, these oral pathogens are related to whole-body systemic diseases[9] including, but not limited to, endocarditis[10] and cardiovascular disease[11,12]. Especially, *P. gingivalis* is well known to play a pivotal role in developing cognitive diseases[13–16].

Astilbe chinensis (Maxim.) Franch. et Savat., from the family Saxifragaceae, is a perennial herbaceous plant that grows in China, Japan's Tsushima Island, northeastern Russia, India, and Korea. In South

Korea, the plant is found all over the country (Fig. 1S). The rhizome of *A. chinensis* has been used for food and medicine to treat headaches and bronchitis, as well as being used as an antipyretic and analgesic remedy[17]. Studies have shown that *A. chinensis* has clinical efficacies, such as regulating adipogenesis[18], and reducing metabolic disorders[19]. Bioactive compounds in *A. chinensis* include astilbic acid[20], astilbin[21], and bergenin[22]. Among them, astilbic acid is well-known to have anti-inflammatory activity in immune cells and animal models[20,23], whereas astilbin has been shown to improve psoriasis in an animal model[24] and prevents osteoarthritis development[25].

While the anti-inflammatory effect of an ethanol extract of *A. chinensis* (ACE)[26] and the rhizomes of *A. chinensis* has been demonstrated[23,27], neither the comparison between its habitats, seasons, and parts (aerial, underground, and inflorescence) of the plant nor the anti-bacterial effect of the ethanol extract on representative oral pathogens have been demonstrated. Here, we for the first time show that the ethanol extract of inflorescence parts of *A. chinensis* gained in a flowering season not only has the most effectiveness in suppressing the activation of inflammatory mediators in LPS-stimulated RAW 264.7 cells, but also can inhibit the growth of important oral pathogens related to periodontal diseases and dental caries.

Methods

Chemicals and Reagents

Dulbecco's modified Eagle's medium (DMEM) and fetal bovine serum (FBS) were purchased from Corning Inc. (Glendale, AZ). Immobilon®-P PVDF membrane, Dimethyl sulfoxide (DMSO), ethylenediaminetetraacetic acid (EDTA), tryptic soy broth, yeast extract, hemin, vitamin K1, LPS (*Escherichia coli* O55:B5), and 3-(4,5-dimethylthiazol-2-yl)-2,5-diphenyltetrazolium bromide (MTT) were from Merck (Darmstadt, Germany). Defibrinated sheep blood was purchased from Synergy innovation (Gyeonggi-do, Korea). Goat anti-mouse IgG (H + L) HRP secondary antibody (Cat. No. 31430), enzyme-linked immunosorbent assay (ELISA) kit, Halt™ protease and phosphatase inhibitor cocktail (100·), RIPA buffer, BD Difco™ Brain Heart Infusion broth, and Griess reagent were purchased from Thermo Fisher Scientific Korea (Seoul, Korea). The antibodies for β-actin (sc-47778), iNOS (NOS2) (sc-7271), COX2 (sc-376861) were from Santa Cruz Biotechnology Inc. (Dallas, TX). Astilbin (Cat. No. S3932) was purchased from Selleck Chemicals (Houston, TX). TRIzol® was from Favorgen (Ping-Tung, Taiwan). BCA assay kit was purchased from Bio-Rad (Hercules, CA).

Collection of A. chinensis samples

Three separate parts of *A. chinensis* plant (aerial parts, rhizomes, and inflorescences) from six separate regions of Republic of Korea (Gapyeong-gun, Gyunggi-do; Yangsan-si, Gyeongsangnam-do; Suncheon-si, Jeollanam-do; Yanggu-gun, Gangwon-do; Gapyeong-gun, Gyunggi-do; Yangsan-si, Gyeongsangnam-do) were collected in flowering and fruiting seasons, which were identified by Dr. Jin-Oh Hyun at Northeastern

Asia Biodiversity Institute (Table 1S). The present study, using wild *A. chinensis*, poses no risk of extinction for the species while complying with national and international guidelines and legislation. Voucher specimens were deposited in the Herbarium of the Bio-Center, Gyeonggido Business & Science Accelerator (GBSA), Suwon, Korea. The total 18 samples were coded respectively from GA-13-1 to GA-13-18. Among them, five samples (GA-13-7, 8, 12, 15, and 17) were excluded based on the initial screening for the sample quality of the plant. Among the 13 selected samples, GA-13-6 showed the most effectiveness in suppressing the inflammatory cytokine IL-6 without cytotoxicity in RAW 264.7 murine macrophages (Fig. 2S).

Preparation of an ethanol extract of A. chinensis **(ACE)**

The dried and powdered samples of each plant system were extracted by maceration with 70% ethanol (1 L per 100 µg of each sample) for 24 h at room temperature. The extract was filtered and evaporated *in vacuo* at 40 ^{o}C, followed by lyophilization. The final extract powders were dissolved in DMSO at a concentration of 100 mg/mL.

Cell culture and viability assay

The RAW 264.7 murine macrophage cell line was obtained from the American Type Culture Collection (ATCC, MD, USA). The cells were cultured at 37°C in DMEM supplemented with 2 mM glutamine, 100 U/mL penicillin, 100 µg/mL streptomycin and 10% fetal bovine serum (FBS) in a 5% CO_2 environment. To evaluate cell viability, RAW 264.7 cells ($3.0{\cdot}10^5$ cells/well) were seeded in a 6-well plate and incubated for 24 h before experimental interventions. The cells were then pre-treated with several concentrations of ACE for 3 or 16 h before treated with 3 µL of LPS solution (100 µg/mL in DMSO) for 3 h. The cells were incubated with MTT solution (5 mg/mL, 200 µL/well) for 3 h at 37°C. The medium was removed and 2 mL of DMSO was added to each well to dissolve the formazan crystals in the viable cells. The optical density was determined at a wavelength of 570 nm using a Multiskan GO (Thermo, USA).

Minimum inhibitory concentration (MIC) assay of oral pathogenic bacteria

Stains of *S. sanguinis* (KCOM 1070), *S. mutans* (KCOM 1054) and *P. gingivalis* (KCOM 2796) were obtained from Korean Collection for Oral Microbiology (KCOM). *P. gingivalis* maintained in KCOM broth supplemented with 5 mg/mL hemin, 1 µg/mL vitamin K1 and 50 mg/mL sterile defibrinated sheep blood. Anaerobic conditions (80% N_2, 10% CO_2, 10% H_2) were used for culture at 37°C for seven days. *S. sanguinis* and *S. mutans* strains were grown in brain heart infusion (BHI) medium at 37°C under anaerobic conditions. Following the inoculation of each single colony in KCOM or BHI liquid medium, anaerobic culture was performed for 24 h to prepare freshly saturated culture medium. For the MIC assay, the initial optical density at 600 nm (OD_{600}) was adjusted to 0.05 in a 6-well plate using the freshly saturated seven-day (*P. gingivalis*) or 24-h (*S. mutans* and *S. sanguinis*) culture. The cells were then treated with GA-13-6 stock (5 mg/mL in ethanol) ranging from 0.008 mg/mL to 1.0 mg/mL in final

concentration and incubated for five to seven days (*P. gingivalis*) and 12–24 h (*S. mutans and S. sanguinis*) before OD_{600} measurement.

Measurement of NO and inflammatory cytokines

RAW 264.7 macrophages at a density of $3.0{\cdot}10^5$ cells/well were seeded in six-well plates for 24 h before experimental interventions. The cells well then pre-treated with several concentrations of ACE for 3 or 16 h before treated with LPS for 3 h. Culture media was collected and centrifuged at 13,000 rpm for 3 min at 4°C. NO in the culture medium was assayed by the Griess reaction as a method of an analysis of nitrite (NO_2^-) with an absorbance at 548 nm. Briefly, 150 µL of cell culture medium was added to each well of a 96-well plate. After the addition of 130 µL of distilled water and 20 µL of Griess reagent (1% sulfanilamide and 0.1% naphthylenediamine dihydrochloride in 2% phosphoric acid), the plate was left for 10 min at room temperature while shaking. The quantification of nitrite production was made spectrophotometrically using an automated colorimetric procedure using a microplate reader (Multiskan GO, Thermo Fisher Scientific, CA, USA). The presence of TNF and IL-6 was measured using an ELISA kit according to the manufacturer's protocol.

Western blotting analysis

Proteins were harvested with RIPA buffer containing Halt™ protease and phosphatase inhibitor, and 0.5 M EDTA solution. Protein concentrations were measured using BCA assay kit. Cell lysates containing 20 µg of protein was loaded onto 10% gels and transferred to a PVDF membrane. The membrane was blocked with 5% skim milk solution and incubated with primary antibody overnight at 4°C. After washing and blocking the membrane, secondary antibody, diluted 1:5,000 in 5% skim milk, was used for 1 h. Bands were detected by ChemiDoc™ Imaging System (Bio-Rad, CA, USA).

cDNA synthesis and qPCR

RNA was extracted from cells, that were then washed once with 1·PBS and prolonged by TRIzol®. Prime Script 1st strand cDNA Synthesis Kit (Takara, Japan) was used for reverse transcription of RNA, and qPCR was carried out using Power SYBR Green PCR Master mix (Applied Biosystems, USA) with Exicycler 96 system (Bioneer, Korea). The following primers (Bioneer, Korea) were used. *Nos2* mRNA analysis: forward 5'-ACATCGACCCGTCCACAGTAT-3' and reverse 5'-CAGAGGGGTAGGCTTGTCTC-3'. *Cox2* mRNA analysis: forward 5'-CTGGTGCCTGGTCTGATGATGTATG-3' and reverse 5'-TCTCCTATGAGTATGAGTCTGCTGGTT-3'. *Gapdh* mRNA analysis: forward 5'-ACCCAGAAGACTGTGGATGG-3' and reverse 5'-CACATTGGGGGTAGGAACAC-3'.

Statistical analysis

Prism 5.0 software for Windows (GraphPad Software, USA) was used to carry out statistical analyses. The data are presented as the mean ± SD of three independent experiments. A two-tailed *t*-test was used to compare means between two groups.

Results

GA-13-6 had no adverse effect on cell viability of LPS-stimulated RAW 264.7 cells

LPS is a dominant element of endotoxins found in Gram-negative bacterial outer membrane that summons inflammatory mediators and cytokines by binding to Toll-like receptor 4 (TLR4)[28]. To efficiently induce inflammatory responses in RAW 264.7 cells, we first optimized the duration of LPS treatment and the concentration of LPS. In prior, we confirmed that IL-6 was induced the most while the cell viability was rarely affected when the cells were pre-treated with 0.3 μg/mL of LPS for 3 h (Fig. 3S). Next, to evaluate the cytotoxicity due to long-term treatment, we used various concentrations of GA-13-6 for the pre-treatment of cells for 3 h (short-term) and 16 h (long-term) before LPS treatment for 3 h. The results showed no significant cytotoxicity when the cells were pre-treated with GA-13-6 up to 200 μg/mL (Fig. 1).

GA-13-6 reduces proinflammatory mediators in LPS-induced RAW 264.7 macrophages

We next evaluated the anti-inflammatory activity of GA-13-6 by observing the suppression of inflammatory indicators in the macrophages. When we used 0.3 μg/mL of LPS for 3 h to induce RAW 264.7 cells, we could observe the induction of proinflammatory cytokines, such as IL-6 (Fig. 2a), TNF (Fig. 2b), and NO (Fig. 2c) in RAW 264.7 cells. However, when the cells were pre-treated with GA-13-6 for either 3 or 16 h, the inductions were suppressed in a dose-dependent manner. In the cases of IL-6 and TNF, the shorter the cells were pre-exposed to GA-13-6, the greater the degree of reduction, while the degree of IL-6 reduction was greater than that of TNF (Fig. 2a and 2b). By contrast, the level of NO production was higher when the cells were pre-treated with GA-13-6 for 16 h before LPS stimulation (Fig. 2c), resulting in a more drastic NO reduction in a dose-dependent manner. Altogether, GA-13-6 pre-treatment successfully prevented RAW 264.7 macrophages from activation of proinflammatory cytokines when the cells were induced by LPS.

GA-13-6 reduced the mRNA and protein expression levels of COX2 and iNOS

Both COX2 and iNOS (NOS2) are known as crucial factors associated with the generation of NO in inflammatory reactions[29]. To determine whether GA-13-6 inhibits the production of NO and inflammatory cytokines through the regulation of COX2 and iNOS expression in RAW 264.7 cells, we analyzed the mRNA expression levels of both *Cox2* and *Nos2* in RAW 264.7 cells. As a result, the mRNA expression levels of both genes were significantly suppressed at concentrations above 25 μg/mL of GA-13-6 with either 3 or 16 h pre-treatment (Fig. 3a and 3b). Of note, similar to the NO production pattern shown in Fig. 2c, the degrees of mRNA expression levels of both genes by LPS stimulation were greater when the macrophages were pre-treated with GA-13-6 for 16 h, resulting in a stiffer reduction of the mRNA expression levels in a dose-dependent manner.

We then confirmed that the protein expression levels of COX2 and iNOS decreased when the RAW 264.7 macrophages were pre-treated with GA-13-6 by Western blotting analysis (Fig. 3c and Fig. 4S). When the macrophages were stimulated by LPS, iNOS was over-expressed that later decreased as the pre-treated concentration of GA-13-6 increased. The degree of iNOS reduction was greater when the cells were pre-treated with GA-13-6 for 3 h. Interestingly, the iNOS expression was slightly upregulated when the cells were pre-treated with 25 μg/mL of GA-13-6, suggesting that there could be a temporal difference between the number of actual proteins translated and the mRNA transcribed in the nucleus. On the other hand, the level of COX2 overexpression was not obvious when the cells were induced by LPS, while the degree of reduction was greater for the cells pre-treated with GA-13-6 for 16 h. The overall expression levels of both iNOS and COX2 were higher when the macrophages were pre-treated with GA-13-6 for 16 h, which agrees with the higher transcription levels of both mRNAs for the samples pre-treated for a longer period (See Fig. 3a and 3b).

Astilbin showed limited efficacy in the prevention of the immune responses in LPS-stimulated RAW 264.7 cells

We next evaluated the anti-inflammatory effect of astilbin, a representative bioactive compound found in *A. chinensis* rhizome[21]. The purified astilbin showed marginal cytotoxicity when the compound was applied to RAW 264.7 macrophages up to 40 μg/mL for 3 and 16 h, respectively (Fig. 4a). Unlike GA-13-6, however, the chemical failed to reduce the activation of IL-6 and TNF (Fig. 4b and 4c). On the contrary, the mRNA expression levels of *Cox2* and *Nos2* in LPS-induced cells were significantly increased when the cells were pre-treated with astilbin (Fig. 4d and 4e). The induction of *Cox2* mRNA was dose-dependent when the cells were pre-treated with astilbin for 3 h, which was disrupted with 16 h (Fig. 4d). By contrast, the induction of *Nos2* mRNA was dose-dependent when the cells were pre-incubated with astilbin for 16 h except the point where 20 μg/mL of astilbin was used (Fig. 4e). Both mRNA expressions were efficiently suppressed only when the macrophages were pre-incubated with 20 μg/mL of astilbin for 16 h, indicating that there could be a narrow window of optimal concentrations and pre-incubation time for this specific chemical to be effective.

GA-13-6 inhibited the growth of major oral pathogenic bacteria

We next demonstrated the antibacterial activity of GA-13-6 by determining minimum inhibitory concentrations (MICs) of three essential oral pathogenic bacteria, *P. gingivalis*, *S. mutans*, and *S. sanguinis*. As a result, we observed that GA-13-6 efficiently inhibited the growth of pathogens in order of *P. gingivalis*, *S. sanguinis*, and *S. mutans* (Fig. 5). While the amount of GA-13-6 was not enough to yield MIC of *S. mutans*, the MICs of *P. gingivalis* and *S. sanguinis* were found to be 0.25 mg/mL and 1.0 mg/mL, respectively.

Discussion

While extracts of *A. chinensis* rhizomes have been frequently reported to have anti-inflammatory[23,27], anti-tumor[30–34], and anti-platelet activities[35], studies on the extract of inflorescence of *A. chinensis* have yet to be reported. In this study, we demonstrated that GA-13-6, an ethanol extract of inflorescence parts of *A. chinensis*, has anti-inflammatory properties as well as antibacterial effect on oral pathogenic bacteria such as *P. gingivalis*, *S. sanguinis*, and *S. mutans*. To that end, we collected three different parts (aerial, underground, inflorescence) of the plant from six different regions of South Korea in two different seasons. The total 18 collected samples were initially screened for sample quality and quantity, followed by preliminary tests for the cell cytotoxicity and anti-IL-6 activity. We chose GA-13-6, an ethanolic extract of *A. chinensis* inflorescence, that inhibited the activation of proinflammatory cytokines most efficiently when RAW 264.7 macrophages were later induced by LPS treatment.

LPS-induced RAW 264.7 macrophages are commonly employed for studies on inflammatory reactions, where NF-κB, a pivotal transcription factor in the nucleus, is activated upon LPS binding to TLR4 on the cell membrane[28,36]. NF-κB plays an important role in regulating the inflammatory responses by boosting the expression of proinflammatory cytokines and inflammatory mediators, such as TNF, IL-6, iNOS, and COX2[37,38]. TNF, a representative inflammatory cytokine, is secreted early in the immune response and is involved in the activation of inflammation and regulation of cell necrosis[39]. IL-6, also produced in the acute phase of inflammatory responses, contributes to host defence in both humoral and cellular immunity[40]. NO, an anti-inflammatory signalling molecule under normal physiological conditions, plays an important role in the pathogenesis of inflammation when over-produced upon infectious and proinflammatory stimuli[41]. In such abnormal situations, iNOS increases to produce more NO by converting L-arginine to L-citrulline[42,43]. NO is also involved in the activation of COX2 that leads to the simultaneous release of mediators, such as prostaglandin E2 (PGE_2) and prostacyclin (PGI_2), from the COX pathway[44,45]. Thus, selective inhibition of the iNOS pathway is an important strategy for controlling many chronic inflammatory diseases including, but not limited to, cognitive and cardiovascular diseases[46]. Especially, when the iNOS synthesis is induced by bacterial endotoxin LPS, the production of high levels of NO is delayed but prolonged[47], partially explaining our Western results where the level of iNOS protein expression is inconsistent with the level of mRNA expression (Fig. 3b and 3c). The reason why the LPS induction of the macrophages should barely increase COX2 protein expression and why the expression levels of both COX2 and iNOS should increase when the macrophages were pre-treated with GA-13-6 for a longer period remain obscure, although the results suggest that GA-13-6 can counteract LPS-mediated immune responses in a dose-dependent manner (Fig. 3c).

Previously, Gil *et al.*[26] demonstrated the anti-inflammatory effect of ACE from the rhizomes of the plant using LPS-stimulated RAW 264.7 macrophages and thioglycollate-elicited peritoneal macrophages from male C57BL/6 mice. They observed a decrease in the levels of inflammatory mediators (NO, iNOS, PGE_2, and COX2) upon pre-incubation of the cells with ACE for 1 h before LPS (1.0 μg/mL) stimulation for over 24 h. In these experimental conditions, the degree of NO reduction was dose-dependent, where 25 μg/mL of ACE was enough to reduce the level of NO to half of the fully elevated level. The expression level of

iNOS followed a similar pattern. The reduction levels of other proinflammatory cytokines (TNF and IL-6), however, were limited and dose-independent. In contrast, we pre-incubated the cells with GA-13-6 for 3 and 16 h to compare the effect of short- and long-term exposure before induction inflammatory responses in RAW 264.7 cells using 0.3 μg/mL of LPS while securing the cell viability. In our experimental conditions, the degrees of reduction of IL-6 and TNF were greater with short-term exposure to GA-13-6 (Fig. 2a and 2b). By contrast, the secretion of NO was greater if the cells were pre-exposed to GA-13-6 for 16 h, resulting in a more drastic decrease as the concentration of GA-13-6 increases (Fig. 2c). Likewise, the mRNA expression levels of both *Cox2* and *Nos2* diminished more stiffly when the cells were exposed for 16 h in a dose-dependent manner. The protein expression levels, however, were remained higher with 16 h pre-treatment of the macrophages with LPS (Fig. 3), indicating that the half-life of the mRNA is shorter than the one of the translated proteins and the longer the incubation the more the protein accumulation. Collectively, GA-13-6 exhibited not less anti-inflammatory effect than ACE from the rhizome in LPS-induced macrophages.

Astilbin is one of the major active flavonoids isolated from the rhizome of *A. chinensis*[48–50] as well as other numerous plants and processed foods like wines, champagnes, and turtle jelly[51]. The anti-inflammatory activity of astilbin has been reported in T helper 17 (Th17) cells in psoriasis-like mouse model[52], HaCaT cells and psoriasis-like guinea pigs model[24], adjuvant-arthritis rat model[48], high glucose-induced glomerular mesangial cells[21], T- and B-cells in lupus mice model[53], mouse J774A.1 macrophages[54], human chondrocytes[25], osteoarthritis mouse[25], and rat models[55]. By contrast, astilbin showed no inhibitory effect on the production of inflammatory mediators and proinflammatory cytokines in LPS-induced RAW 264.7 macrophages (Fig. 4). Interestingly, astilbin isolated from *Smilax corbularia* was reported to have no inhibitory effect on NO production while blocking PGE_2 release in RAW 264.7 cells induced by 1.0 μg/mL of LPS for 24 h[50]. Additionally, astilbin from the rhizome of *Smilax glabra* was reported to inhibit the production of NO and TNF but not IL-6 in RAW 264.7 cells induced by 1.0 μg/mL of LPS for 20 h[49]. Given that flavonoids, commonly found in photosynthesizing plants, possess anti-inflammatory activity in general[51], the inconsistency of the results among the research groups may originate from the differences between cell lines, e.g., RAW 264.7 cells vs others, and the amount and duration of LPS treatment. It should be noted, however, that GA-13-6 comprises a variety of functional flavonoids[17,56] that can together yield stronger anti-inflammatory activity than a single compound can[50].

Periodontal disease is associated with a variety of bacteria and biofilms they form that can cause damages to the periodontal support structure, which is closely related to many systemic diseases[2,57]. *P. gingivalis* is a keystone pathogenic bacterium for the onset of periodontal disease[58]. Recent studies have corroborated the close relationship between the bacterium and systemic diseases including, but not limited to, cancer, cardiovascular disease[59–63], diabetes[64,65], rheumatoid arthritis[66], and Alzheimer's disease[13–16,67–70]. *P. gingivalis* produces several potential virulence factors, such as gingipain proteases, outer membrane vesicles (OMVs), LPS, capsule, and fimbriae[15,16,69–72]. Among them, gingipain proteases (Rgp and Kgp) are required for its survival while serving as primary virulence factors simultaneously[69].

Especially, gingipains are directly involved in the modulation of gene expression associated with dementia in the brain[70]. While capsule and fimbriae mediate physical interactions with host cells, LPS and OMVs trigger intracellular proinflammatory signalling pathways[16,63]. On the other hand, bacterial commensals or opportunistic pathogens, such as *S. sanguinis*, *Streptococcus gordonii*, and *Candida albicans*, may provide *P. gingivalis* with favourable environment for its pathogenesis when a balance of bacterial community disrupted[71]. Given that plant flavonoids could reduce the inflammatory responses and inhibit bacterial growth[73], we assumed that GA-13-6 may contain a variety of flavonoids and could suppress the growth of oral pathogens. As expected, GA-13-6 efficiently inhibit the growth of *P. gingivalis* as well as *S. sanguinis* and *S. mutans*, suggesting that GA-13-6 may prevent infection and suppress ensuing inflammation if any infections occur. The difference in the inhibitory efficacy of GA-13-6 between the Gram-positive and Gram-negative bacteria as shown in Fig. 5 could be due to the difference in membrane structures, which can be disrupted by some flavonoids[74]. Thus, instead of using conventional antibiotics for treatment that can cause dysbiosis and antibiotic resistance, using natural extracts such as GA-13-6 may facilitate the restoration of healthy oral commensalism with minimal side effects.

In this study, we put an effort to collect three different parts of *A. chinensis* from a wide variety of regions in two different seasons and screen the optimal part of the plant that can effectively prevent the onset of cellular inflammation as well as the growth of oral pathogenic bacteria. By following the screening process, we for the first time found that inflorescence of *A. chinensis*, GA-13-6, acquired in a flowering season exhibited the best performance. We sought to employ GA-13-6 as a natural resource for the prevention and remedy of periodontal disease, a near-pandemic disease in oral cavity, and widespread dental caries as well. As expected, GA-13-6 successfully suppressed both cellular inflammation responses and oral bacterial growth. Our previous findings indicated that the aerial part of *A. chinensis* contains nine flavonoids including quercetin but not astilbin[56]. Thus, further study is needed to identify active ingredients of GA-13-6 responsible for the anti-bacterial efficacy and to define the selectivity of GA-13-6 for many other benign and harmful bacteria in oral cavity.

GA-13-6, an ethanol extract from *A. chinensis* inflorescence, efficiently suppressed the activation of proinflammatory cytokines and inflammatory mediators, such as TNF, IL-6, and NO, as well as the expression of COX2 and iNOS enzymes in LPS-stimulated RAW 264.7 macrophages. The anti-inflammatory efficacy of GA-13-6 is greater than the one of purified astilbin, which is one of the major effective ingredients found in *A. chinensis*. The antibacterial effects of the extracts were also confirmed for the first time against key oral pathogens, such as *P. gingivalis, S. sanguinis*, and *S. mutans*, indicating that GA-13-6 can inhibit bacterial infection in the oral cavity and suppress the ensuing inflammatory responses.

Declarations

Acknowledgements

The authors would like to thank Hyun Hye Moon for technical assistance. We also thank Dr. Do-Young Park for critical reading and constructive comments for this paper.

Author contributions

JMH performed the experiments, analyzed the data, and drafted the manuscript. IY and KMY performed the experiments and analyzed the data. WJ and SSH collected the samples and prepared the organic extracts. HSK and YYK organized the project and provided critical decision makings. IH designed the study, analyzed the data, and prepared the manuscript. All authors approved the manuscript to be submitted.

Competing interests

J.M.H., I.Y., K.M.Y., H.-S.K., W.J., S.S.H., and I.H. are inventors on an issued patent filed by ATIBS and GBSA describing the anti-inflammatory and antibacterial effect of an ethanol extract of *A. chinensis* (ROK Pat. No. 10-2231892, registered on 19 Mar. 2021). I.H. is an advisor to ATIBS and has given lectures in symposia sponsored by ATDH. J.M.H. and I.H. are employees of Docsmedi that has a commercial interest in the results.

Additional information

Supplementary Information. The online version contains supplementary material available at https://doi.org/...

References

1. Zero, D. T. *et al.* Clinical practice guidelines for oral management of Sjogren disease: Dental caries prevention. *J. Am. Dent. Assoc*, **147**, 295–305 https://doi.org/10.1016/j.adaj.2015.11.008 (2016).
2. Kinane, D. F., Stathopoulou, P. G. & Papapanou, P. N. Periodontal diseases. *Nat. Rev. Dis. Primers*, **3**, 17038 https://doi.org/10.1038/nrdp.2017.38 (2017).
3. Kolenbrander, P. E. *et al.* Communication among oral bacteria. *Microbiol. Mol. Biol. Rev*, **66**, 486–505 table of contentshttps://doi.org/10.1128/mmbr.66.3.486-505.2002 (2002).
4. Rogers, J. E. *et al.* Actinobacillus actinomycetemcomitans lipopolysaccharide-mediated experimental bone loss model for aggressive periodontitis. *J. Periodontol*, **78**, 550–558 https://doi.org/10.1902/jop.2007.060321 (2007).
5. Golz, L. *et al.* LPS from P. gingivalis and hypoxia increases oxidative stress in periodontal ligament fibroblasts and contributes to periodontitis. *Mediators Inflamm.* 2014, 986264, doi:10.1155/2014/986264 (2014).
6. Terai, T. *et al.* Screening of Probiotic Candidates in Human Oral Bacteria for the Prevention of Dental Disease. *PLoS One*, **10**, e0128657 https://doi.org/10.1371/journal.pone.0128657 (2015).

7. Takahashi, N. & Nyvad, B. The role of bacteria in the caries process: ecological perspectives. *J. Dent. Res*, **90**, 294–303 https://doi.org/10.1177/0022034510379602 (2011).
8. Scharnow, A. M., Solinski, A. E., Wuest, W. M. & Targeting S. mutans biofilms: a perspective on preventing dental caries. *Medchemcomm*, **10**, 1057–1067 https://doi.org/10.1039/c9md00015a (2019).
9. Gao, L. *et al.* Oral microbiomes: more and more importance in oral cavity and whole body. *Protein Cell*, **9**, 488–500 https://doi.org/10.1007/s13238-018-0548-1PMID – 29736705 (2018).
10. Crump, K. E. *et al.* The relationship of the lipoprotein SsaB, manganese and superoxide dismutase in Streptococcus sanguinis virulence for endocarditis. *Mol. Microbiol*, **92**, 1243–1259 https://doi.org/10.1111/mmi.12625 (2014).
11. Lucchese, A. Streptococcus mutans antigen I/II and autoimmunity in cardiovascular diseases. *Autoimmun. Rev*, **16**, 456–460 https://doi.org/10.1016/j.autrev.2017.03.009 (2017).
12. Paul, O., Arora, P., Mayer, M. & Chatterjee, S. Inflammation in Periodontal Disease: Possible Link to Vascular Disease. *Front. Physiol*, **11**, 609614 https://doi.org/10.3389/fphys.2020.609614 (2020).
13. Dominy, S. S. *et al.* Porphyromonas gingivalis in Alzheimer's disease brains: Evidence for disease causation and treatment with small-molecule inhibitors. *Sci. Adv*, **5**, eaau3333 https://doi.org/10.1126/sciadv.aau3333 (2019).
14. Beydoun, M. A. *et al.* Clinical and Bacterial Markers of Periodontitis and Their Association with Incident All-Cause and Alzheimer's Disease Dementia in a Large National Survey. *J. Alzheimers Dis*, **75**, 157–172 https://doi.org/10.3233/JAD-200064 (2020).
15. Nara, P. L., Sindelar, D., Penn, M. S., Potempa, J. & Griffin, W. S. T. Porphyromonas gingivalis Outer Membrane Vesicles as the Major Driver of and Explanation for Neuropathogenesis, the Cholinergic Hypothesis, Iron Dyshomeostasis, and Salivary Lactoferrin in Alzheimer's Disease. *J. Alzheimers Dis*, 1–34 https://doi.org/10.3233/jad-210448PMID – 34275903 (2021).
16. Zhang, Z., Liu, D., Liu, S., Zhang, S. & Pan, Y. The Role of Porphyromonas gingivalis Outer Membrane Vesicles in Periodontal Disease and Related Systemic Diseases. *Front. Cell. Infect. Microbiol*, **10**, 585917 https://doi.org/10.3389/fcimb.2020.585917PMID – 33585266 (2021).
17. Xue, Y., Xu, X. M., Yan, J. F., Deng, W. L. & Liao, X. Chemical constituents from Astilbe chinensis. *J. Asian Nat. Prod. Res*, **13**, 188–191 https://doi.org/10.1080/10286020.2010.546355 (2011).
18. Zhang, X. H. *et al.* Antiobesity Effect of Astilbe chinensis Franch. et Savet. Extract through Regulation of Adipogenesis and AMP-Activated Protein Kinase Pathways in 3T3-L1 Adipocyte and High-Fat Diet-Induced C57BL/6N Obese Mice. *Evid. Based Complement. Alternat. Med.* 2018, 1347612, doi:10.1155/2018/1347612 (2018).
19. Sancheti, S., Sancheti, S., Lee, S. H., Lee, J. E. & Seo, S. Y. Screening of Korean Medicinal Plant Extracts for alpha-Glucosidase Inhibitory Activities. *Iran. J. Pharm. Res*, **10**, 261–264 (2011).
20. Yuk, J. E. *et al.* Effects of astilbic acid on airway hyperresponsiveness and inflammation in a mouse model of allergic asthma. *Int. Immunopharmacol*, **11**, 266–273 https://doi.org/10.1016/j.intimp.2010.12.002 (2011).

21. Chen, F., Zhu, X., Sun, Z. & Ma, Y. Astilbin Inhibits High Glucose-Induced Inflammation and Extracellular Matrix Accumulation by Suppressing the TLR4/MyD88/NF-kappaB Pathway in Rat Glomerular Mesangial Cells. *Front. Pharmacol*, **9**, 1187 https://doi.org/10.3389/fphar.2018.01187 (2018).
22. Chen, W. D. & Nie, M. H. HPLC determination of bergenin in Astilbe chinensis (Maxim.) Franch. et Sav. and Bergenia purpurascens (Hook. F. et Thoms.) Engl. *Yao Xue Xue Bao*, **23**, 606–609 (1988).
23. Moon, T. C. *et al.* Antiinflammatory activity of astilbic acid from Astilbe chinensis. *Biol. Pharm. Bull*, **28**, 24–26 https://doi.org/10.1248/bpb.28.24 (2005).
24. Yu, J., Xiao, Z., Zhao, R., Lu, C. & Zhang, Y. Astilbin emulsion improves guinea pig lesions in a psoriasis-like model by suppressing IL-6 and IL-22 via p38 MAPK. *Mol. Med. Rep*, **17**, 3789–3796 https://doi.org/10.3892/mmr.2017.8343 (2018).
25. Sun, S. *et al.* Astilbin prevents osteoarthritis development through the TLR4/MD-2 pathway. *J. Cell. Mol. Med*, **24**, 13104–13114 https://doi.org/10.1111/jcmm.15915 (2020).
26. Gil, T. Y., Jin, B. R., Hong, C. H., Park, J. H. & An, H. J. Astilbe Chinensis ethanol extract suppresses inflammation in macrophages via NF-kappaB pathway. *BMC Complement. Med. Ther*, **20**, 302 https://doi.org/10.1186/s12906-020-03073-5 (2020).
27. Na, M. *et al.* Effect of the rhizomes of Astilbe chinensis on UVB-induced inflammatory response. *Phytother. Res*, **18**, 1000–1004 https://doi.org/10.1002/ptr.1599 (2004).
28. Lucas, K. & Maes, M. Role of the Toll Like receptor (TLR) radical cycle in chronic inflammation: possible treatments targeting the TLR4 pathway. *Mol. Neurobiol*, **48**, 190–204 https://doi.org/10.1007/s12035-013-8425-7 (2013).
29. Murakami, A., Ohigashi, H., Targeting, N. O. X., INOS & and COX-2 in inflammatory cells: Chemoprevention using food phytochemicals. *Int. J. Cancer*, **121**, 2357–2363 https://doi.org/10.1002/ijc.23161 (2007).
30. Tu, J., Sun, H. X. & Ye, Y. P. Immunomodulatory and antitumor activity of triterpenoid fractions from the rhizomes of Astilbe chinensis. *J. Ethnopharmacol*, **119**, 266–271 https://doi.org/10.1016/j.jep.2008.07.007 (2008).
31. Sun, H. X., Zheng, Q. F. & Tu, J. Induction of apoptosis in HeLa cells by 3beta-hydroxy-12-oleanen-27-oic acid from the rhizomes of Astilbe chinensis. *Bioorg. Med. Chem*, **14**, 1189–1198 https://doi.org/10.1016/j.bmc.2005.09.043 (2006).
32. Sun, H. X., Ye, Y. P. & Pan, Y. J. Cytotoxic oleanane triterpenoids from the rhizomes of Astilbe chinensis (Maxim.) Franch. et Savat. *J. Ethnopharmacol*, **90**, 261–265 https://doi.org/10.1016/j.jep.2003.10.003 (2004).
33. Cai, X. F. *et al.* Cytotoxic triterpenoids from the rhizomes of Astilbe chinensis. *J. Nat. Prod*, **72**, 1241–1244 https://doi.org/10.1021/np900028v (2009).
34. Deng, W., Sun, H. X., Chen, F. Y. & Yao, M. L. Immunomodulatory activity of 3beta,6beta-dihydroxyolean-12-en-27-oic acid in tumor-bearing mice. *Chem. Biodivers*, **6**, 1243–1253 https://doi.org/10.1002/cbdv.200800187 (2009).

35. Jeon, B. R., Irfan, M., Lee, S. E., Lee, J. H. & Rhee, M. H. Astilbe chinensis Modulates Platelet Function via Impaired MAPK and PLCgamma2 Expression. Evid. Based Complement. Alternat. Med. 2018, 3835021, doi:10.1155/2018/3835021 (2018).
36. Chow, J. C., Young, D. W., Golenbock, D. T., Christ, W. J. & Gusovsky, F. Toll-like receptor-4 mediates lipopolysaccharide-induced signal transduction. *J. Biol. Chem*, **274**, 10689–10692 https://doi.org/10.1074/jbc.274.16.10689 (1999).
37. Tak, P. P. & Firestein, G. S. NF-kappaB: a key role in inflammatory diseases. *J. Clin. Invest*, **107**, 7–11 https://doi.org/10.1172/JCI11830 (2001).
38. Kanno, S. *et al.* Inhibitory effect of naringin on lipopolysaccharide (LPS)-induced endotoxin shock in mice and nitric oxide production in RAW 264.7 macrophages. *Life Sci*, **78**, 673–681 https://doi.org/10.1016/j.lfs.2005.04.051 (2006).
39. Fischer, R. & Maier, O. Interrelation of oxidative stress and inflammation in neurodegenerative disease: role of TNF. Oxid. Med. Cell. Longev. 2015, 610813, doi:10.1155/2015/610813 (2015).
40. Tanaka, T., Narazaki, M. & Kishimoto, T. IL-6 in inflammation, immunity, and disease. *Cold Spring Harb. Perspect. Biol*, **6**, a016295 https://doi.org/10.1101/cshperspect.a016295 (2014).
41. Sharma, J. N., Al-Omran, A. & Parvathy, S. S. Role of nitric oxide in inflammatory diseases., **15**, 252–259 https://doi.org/10.1007/s10787-007-0013-x (2007).
42. Weinberg, J. B. *et al.* Human mononuclear phagocyte inducible nitric oxide synthase (iNOS): analysis of iNOS mRNA, iNOS protein, biopterin, and nitric oxide production by blood monocytes and peritoneal macrophages., **86**, 1184–1195 (1995).
43. Schwedhelm, E. *et al.* Pharmacokinetic and pharmacodynamic properties of oral L-citrulline and L-arginine: impact on nitric oxide metabolism. *Br. J. Clin. Pharmacol*, **65**, 51–59 https://doi.org/10.1111/j.1365-2125.2007.02990.x (2008).
44. Salvemini, D. *et al.* Nitric oxide activates cyclooxygenase enzymes. *Proc. Natl. Acad. Sci. U.S.A.* **90**, 7240–7244, doi:10.1073/pnas.90.15.7240 (1993).
45. Ahmad, N., Chen, L. C., Gordon, M. A., Laskin, J. D. & Laskin, D. L. Regulation of cyclooxygenase-2 by nitric oxide in activated hepatic macrophages during acute endotoxemia. *J. Leukoc. Biol*, **71**, 1005–1011 (2002).
46. Vanhatalo, A. *et al.* Network analysis of nitrate-sensitive oral microbiome reveals interactions with cognitive function and cardiovascular health across dietary interventions. *Redox Biol*, **41**, 101933 https://doi.org/10.1016/j.redox.2021.101933 (2021).
47. Salvemini, D., Kim, S. F. & Mollace, V. Reciprocal regulation of the nitric oxide and cyclooxygenase pathway in pathophysiology: relevance and clinical implications. *Am. J. Physiol. Regul Integr. Comp. Physiol*, **304**, R473–487 https://doi.org/10.1152/ajpregu.00355.2012 (2013).
48. Dong, L. *et al.* Astilbin from Smilax glabra Roxb. Attenuates Inflammatory Responses in Complete Freund's Adjuvant-Induced Arthritis Rats. *Evid. Based Complement. Alternat. Med.* 2017, 8246420, doi:10.1155/2017/8246420 (2017).

49. Lu, C. L. *et al.* Optimization of astilbin extraction from the rhizome of Smilax glabra, and evaluation of its anti-inflammatory effect and probable underlying mechanism in lipopolysaccharide-induced RAW264.7 macrophages., **20**, 625–644 https://doi.org/10.3390/molecules20010625 (2015).
50. Ruangnoo, S. *et al.* An in vitro inhibitory effect on RAW 264.7 cells by anti-inflammatory compounds from Smilax corbularia Kunth. *Asian Pac. J. Allergy Immunol*, **30**, 268–274 (2012).
51. Sharma, A. *et al.* A Promising Unexplored Compound with Multidimensional Medicinal and Health Benefits. *Pharmacol. Res*, **158**, 104894 https://doi.org/10.1016/j.phrs.2020.104894 (2020).
52. Di, T. T. *et al.* Astilbin inhibits Th17 cell differentiation and ameliorates imiquimod-induced psoriasis-like skin lesions in BALB/c mice via Jak3/Stat3 signaling pathway. *Int. Immunopharmacol*, **32**, 32–38 https://doi.org/10.1016/j.intimp.2015.12.035 (2016).
53. Guo, L. *et al.* Decrease of Functional Activated T and B Cells and Treatment of Glomerulonephitis in Lupus-Prone Mice Using a Natural Flavonoid Astilbin. *PLoS One*, **10**, e0124002 https://doi.org/10.1371/journal.pone.0124002 (2015).
54. Huang, H. *et al.* Isolation and characterization of two flavonoids, engeletin and astilbin, from the leaves of Engelhardia roxburghiana and their potential anti-inflammatory properties. *J. Agric. Food Chem*, **59**, 4562–4569 https://doi.org/10.1021/jf2002969 (2011).
55. Chen, C. *et al.* Astilbin-induced inhibition of the PI3K/AKT signaling pathway decelerates the progression of osteoarthritis. *Exp. Ther. Med*, **20**, 3078–3083 https://doi.org/10.3892/etm.2020.9048 (2020).
56. Seo, C. *et al.* Flavonoids from the Aerial Parts of Astilbe rubra. *Chem. Nat. Compd*, **55**, 1153–1155 https://doi.org/10.1007/s10600-019-02919-w (2019).
57. Genco, R. J. & Sanz, M. Clinical and public health implications of periodontal and systemic diseases: An overview. *Periodontol. 2000*, **83**, 7–13 https://doi.org/10.1111/prd.12344 (2020).
58. How, K. Y., Song, K. P. & Chan, K. G. Porphyromonas gingivalis: An Overview of Periodontopathic Pathogen below the Gum Line. *Front. Microbiol*, **7**, 53 https://doi.org/10.3389/fmicb.2016.00053 (2016).
59. Chou, H. H. *et al.* Porphyromonas gingivalis fimbria-dependent activation of inflammatory genes in human aortic endothelial cells. *Infect. Immun*, **73**, 5367–5378 https://doi.org/10.1128/IAI.73.9.5367-5378.2005 (2005).
60. Khlgatian, M., Nassar, H., Chou, H. H., Gibson, F. C., Genco, C. A. & 3rd & Fimbria-dependent activation of cell adhesion molecule expression in Porphyromonas gingivalis-infected endothelial cells. *Infect. Immun*, **70**, 257–267 https://doi.org/10.1128/IAI.70.1.257-267.2002 (2002).
61. Takahashi, Y., Davey, M., Yumoto, H., Gibson, F. C., Genco, C. A. & 3rd & Fimbria-dependent activation of pro-inflammatory molecules in Porphyromonas gingivalis infected human aortic endothelial cells. *Cell. Microbiol*, **8**, 738–757 https://doi.org/10.1111/j.1462-5822.2005.00661.x (2006).
62. Bengtsson, T. *et al.* The periodontal pathogen Porphyromonas gingivalis cleaves apoB-100 and increases the expression of apoM in LDL in whole blood leading to cell proliferation. *J. Intern. Med*, **263**, 558–571 https://doi.org/10.1111/j.1365-2796.2007.01917.x (2008).

63. Yumoto, H. *et al.* Sensitization of human aortic endothelial cells to lipopolysaccharide via regulation of Toll-like receptor 4 by bacterial fimbria-dependent invasion. *Infect. Immun*, **73**, 8050–8059 https://doi.org/10.1128/IAI.73.12.8050-8059.2005 (2005).
64. Ojima, M. *et al.* Relationship of periodontal bacterium genotypic variations with periodontitis in type 2 diabetic patients., **28**, 433–434 https://doi.org/10.2337/diacare.28.2.433 (2005).
65. Tian, J. *et al.* Porphyromonas gingivalis Induces Insulin Resistance by Increasing BCAA Levels in Mice. *J. Dent. Res*, **99**, 839–846 https://doi.org/10.1177/0022034520911037 (2020).
66. Perricone, C. *et al.* Porphyromonas gingivalis and rheumatoid arthritis. *Curr. Opin. Rheumatol*, **31**, 517–524 https://doi.org/10.1097/BOR.0000000000000638 (2019).
67. Singhrao, S. K. & Olsen, I. Assessing the role of Porphyromonas gingivalis in periodontitis to determine a causative relationship with Alzheimer's disease. *J. Oral Microbiol*, **11**, 1563405 https://doi.org/10.1080/20002297.2018.1563405 (2019).
68. Poole, S. *et al.* Active invasion of Porphyromonas gingivalis and infection-induced complement activation in ApoE-/- mice brains. *J. Alzheimers Dis*, **43**, 67–80 https://doi.org/10.3233/JAD-140315 (2015).
69. Guo, Y., Nguyen, K. A. & Potempa, J. Dichotomy of gingipains action as virulence factors: from cleaving substrates with the precision of a surgeon's knife to a meat chopper-like brutal degradation of proteins. *Periodontol. 2000*, **54**, 15–44 https://doi.org/10.1111/j.1600-0757.2010.00377.x (2010).
70. Patel, S. *et al.* Characterization of Human Genes Modulated by Porphyromonas gingivalis Highlights the Ribosome, Hypothalamus, and Cholinergic Neurons. *Front. Immunol*, **12**, 646259 https://doi.org/10.3389/fimmu.2021.646259 (2021).
71. Lunar Silva, I. & Cascales, E. Molecular Strategies Underlying Porphyromonas gingivalis Virulence. *J. Mol. Biol*, **433**, 166836 https://doi.org/10.1016/j.jmb.2021.166836 (2021).
72. Gui, M. J., Dashper, S. G., Slakeski, N., Chen, Y. Y. & Reynolds, E. C. Spheres of influence: Porphyromonas gingivalis outer membrane vesicles. *Mol. Oral Microbiol*, **31**, 365–378 https://doi.org/10.1111/omi.12134 (2016).
73. Farhadi, F., Khameneh, B., Iranshahi, M. & Iranshahy, M. Antibacterial activity of flavonoids and their structure-activity relationship: An update review. *Phytother. Res*, **33**, 13–40 https://doi.org/10.1002/ptr.6208 (2019).
74. Górniak, I., Bartoszewski, R. & Króliczewski, J. Comprehensive review of antimicrobial activities of plant flavonoids. *Phytochem. Rev*, **18**, 241–272 https://doi.org/10.1007/s11101-018-9591-z (2019).

Figures

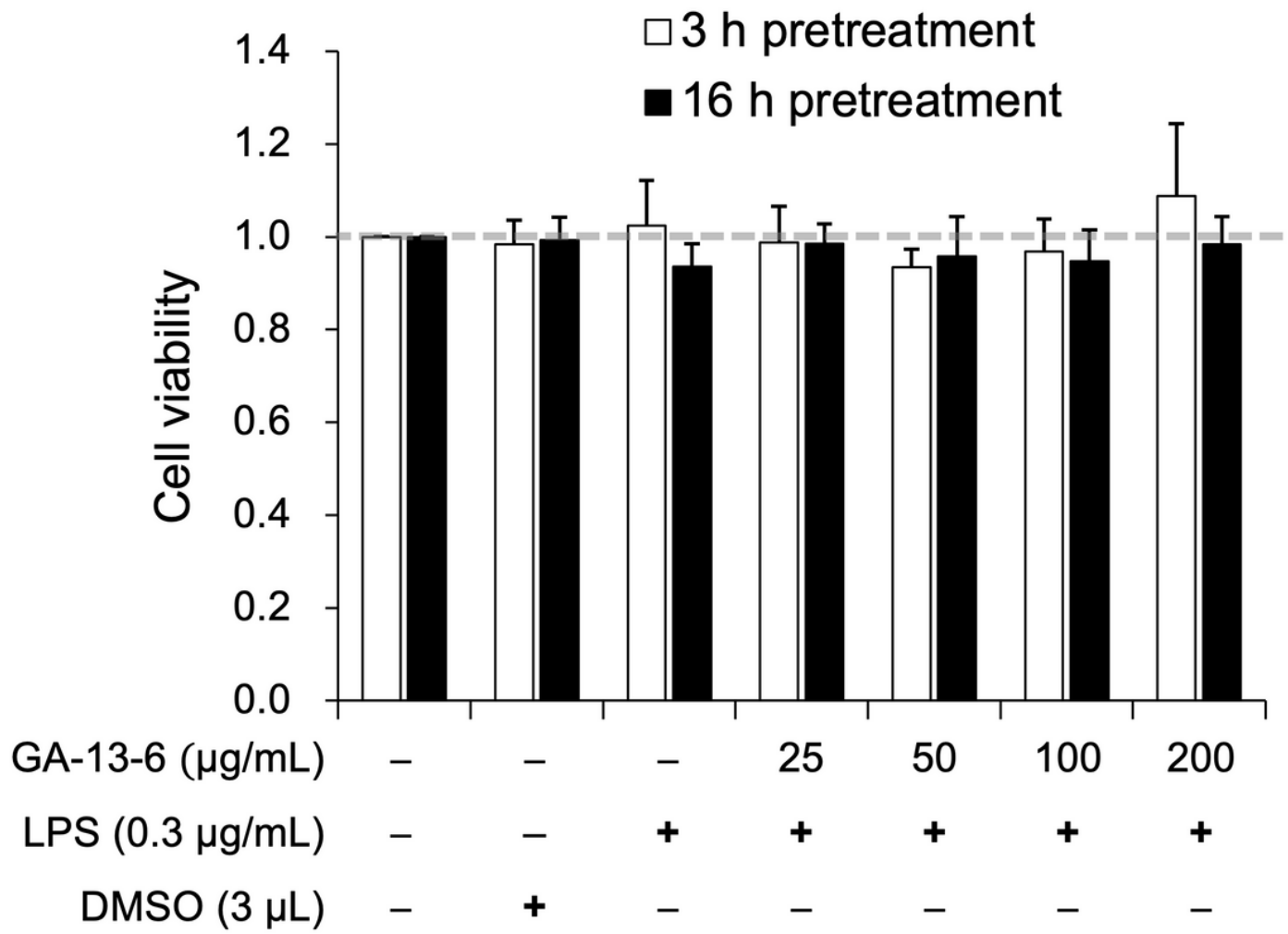

Figure 1

Effect of GA-13-6 on cell viability of LPS-induced RAW 264.7 cells. The cells were pre-treated with GA-13-6 (0, 25, 50,100, 200 μg/mL) for 3 h (empty bars) and 16 h (filled bars), respectively, prior to LPS (0.3 μg/mL) treatment for 3 h. The cell proliferation was estimated by MTT assay.

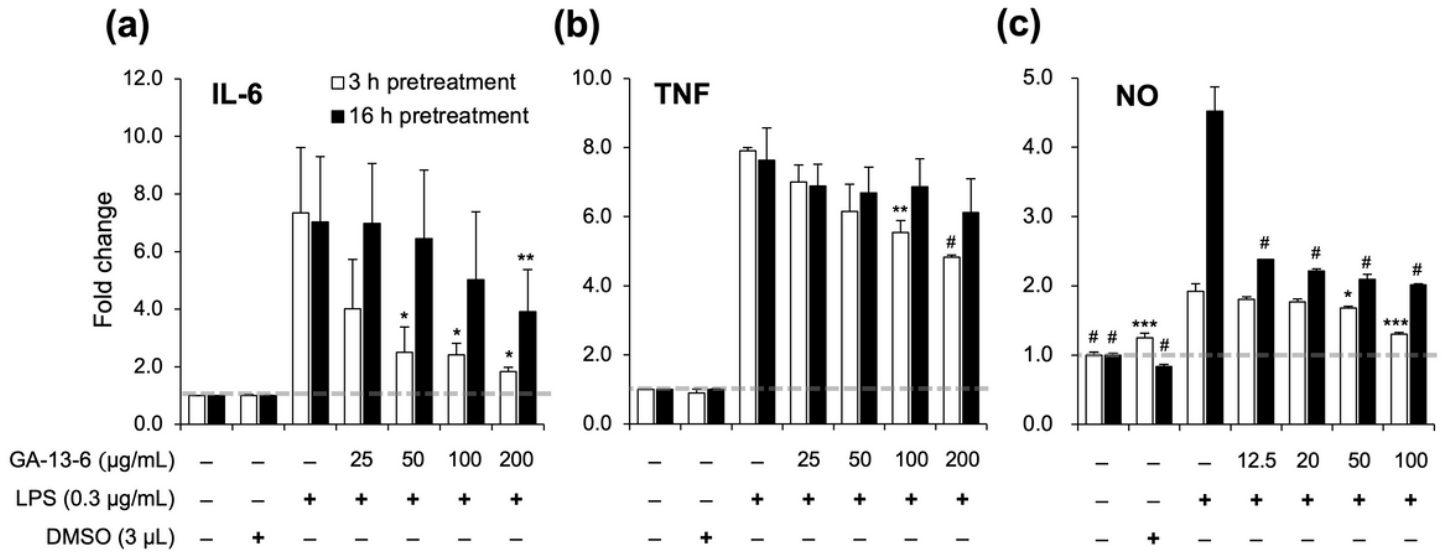

Figure 2

Effect of GA-13-6 on the production of proinflammatory mediators in LPS-induced RAW 264.7 cells. The effects of pre-treatment with GA-13-6 for 3 h (empty bars) or 16 h (filled bars) on LPS (0.3 μg/mL)-induced proinflammatory cytokines were shown. The released amounts of IL-6 (a), TNF (b), and NO (c) were normalized by cells only control to compare the level of stimulation by LPS. *p < 0.05, **p < 0.01, ***p < 0.005, #p < 0.001; unpaired t-test vs LPS only control group.

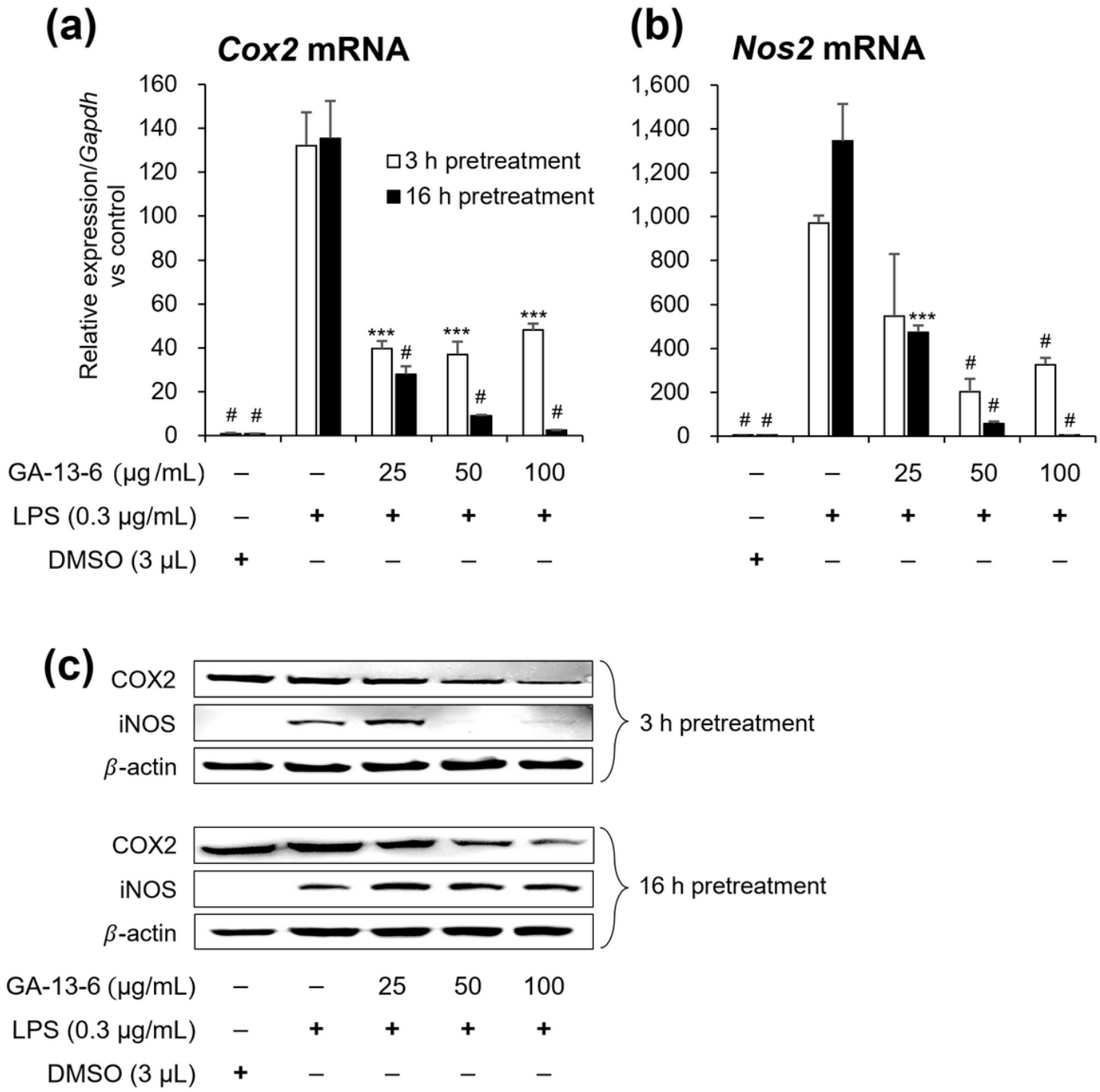

Figure 3

Effect of GA-13-6 on mRNA and protein expression levels of COX2 and iNOS in LPS-induced RAW 264.7 cells. The cells were pre-treated with GA-13-6 (0, 25, 50,100 μg/mL) for 3 h (empty bars) and 16 h (filled bars), respectively, before incubation with LPS (0.3 μg/mL) for 3 h. The mRNA expression levels of Cox2 (a) and Nos2 (b) were normalized using Gapdh gene. Protein expression levels of COX2 and iNOS (c) were confirmed by Western blotting. ***p < 0.005; #p < 0.001; unpaired t-test vs LPS only control group.

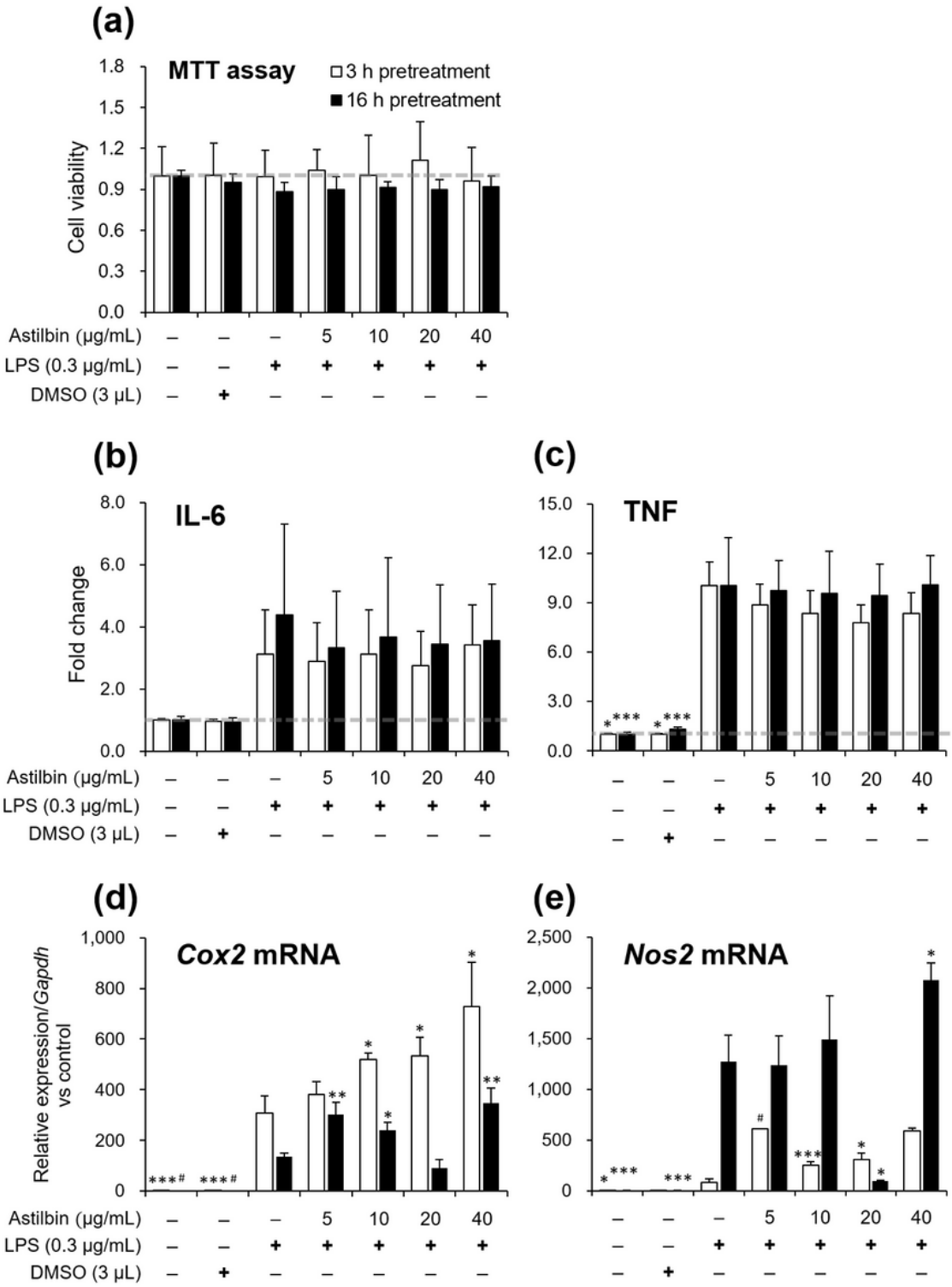

Figure 4

Effect of astilbin on cell viability of LPS-induced RAW 264.7 cells. The cells were pre-treated with astilbin (0, 5, 10, 20, 40 μg/mL) for 3 h (empty bars) and 16 h (filled bars), respectively, prior to LPS (0.3 μg/mL) treatment for 3 h. The cell proliferation was measured by MTT assay (a). The expression levels of IL-6 (b) and TNF (c) were determined by ELISA. The mRNA expression levels of Cox2 (d) and Nos2 (e) were

normalized using Gapdh gene. *p < 0.05, **p < 0.01, ***p < 0.005, #p < 0.001; unpaired t-test vs LPS only control group.

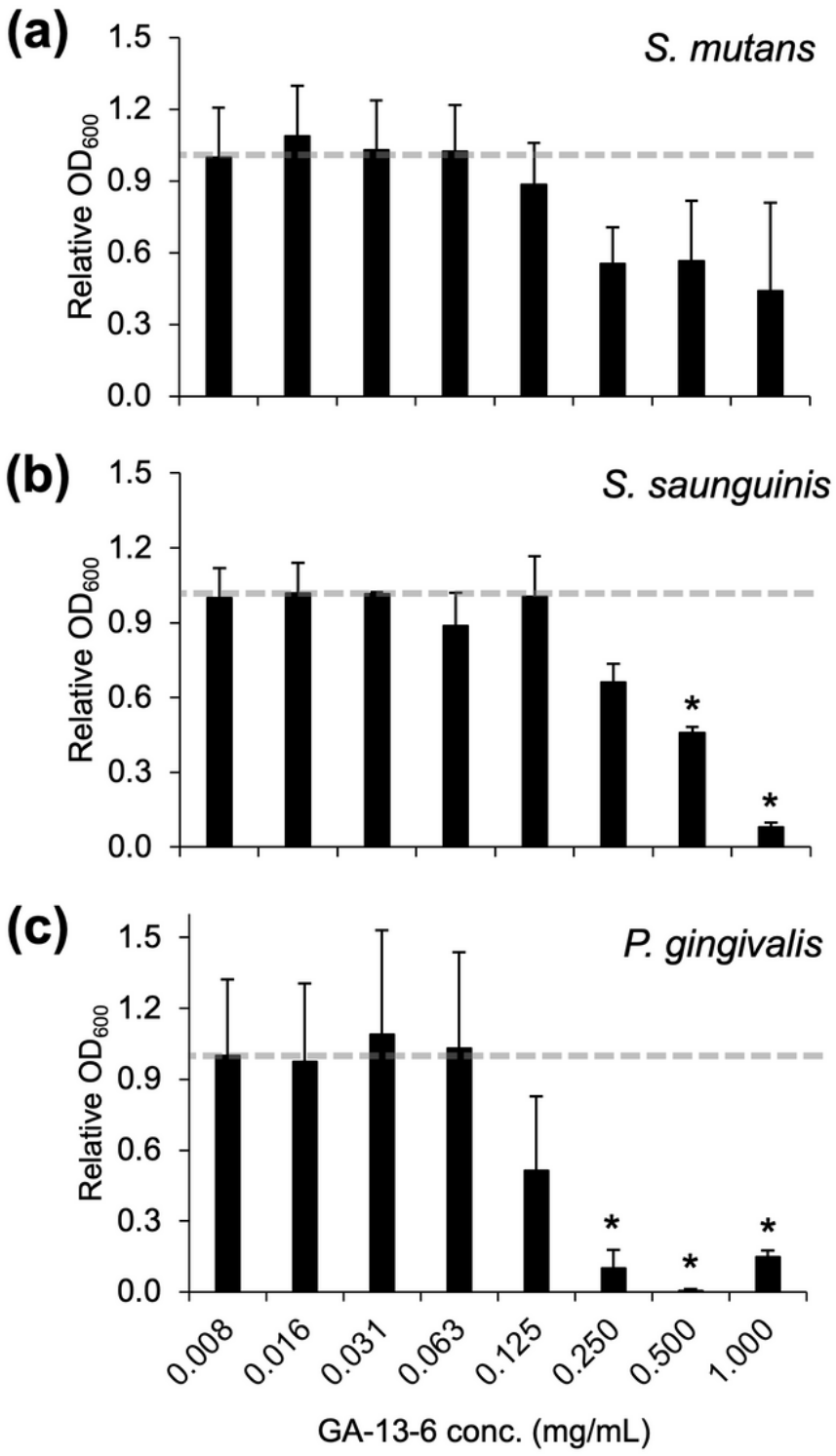

Figure 5

Antibacterial effect of GA-13-6 on oral key pathogens. GA-13-6 inhibited most strongly the growth of P. gingivalis, followed by S. sanguinis and S. mutans. Bacterial cell viability was determined by normalized OD600. *p < 0.05; unpaired t-test vs the minimum GA-13-6 concentration group.

Supplementary Files

This is a list of supplementary files associated with this preprint. Click to download.

- AstilbechinensisSRSI.pdf